ISBN: 978-3-95450-233-2 ISSN: 2673-5504 doi:10.18429/JACoW-SRF2021-SUPFDV012

THE DEVELOPMENT OF HiPIMS MULTILAYER SIS FILM COATINGS ON COPPER FOR SRF APPLICATIONS

S. Leith†[1], M. Vogel[1], E. Seiler[2], R, Ries[2], Y. Li[3], J. Müller[3], D. Tikhonov[4], O. Kugeler[4], S. Keckert[4], A. Ö. Sezgin[1], X. Jiang[1], B. Butz[3], J. Knobloch[4,5]
[1]Institute of Materials Engineering, University of Siegen, Siegen, Germany
[2]Institute of Electrical Engineering SAS, Bratislava, Slovakia
[3]Micro- and Nanoanalytics Group, University of Siegen, Germany
[4]Helmholtz-Zentrum Berlin für Materialen und Energie GmbH, Germany
[5]Department of Physics, University of Siegen, Germany

Abstract

In recent years, the use of alternatives to bulk Nb in the fabrication of SRF cavities, including novel materials and/or fabrication techniques, have been extensively explored by the SRF community. One of these new methodologies is the use of a superconductor-insulator-superconductor (SIS) multilayer structure. Typically, these have been envisaged for use with bulk Nb cavities. However, it is conceivable to combine the benefits of SIS structures with the benefits of coated Cu cavities, such as operation at 4.2 K. It is also clear that the use of, so-called, energetic deposition techniques such as high power impulse magnetron sputtering (HiPIMS), provide significant benefits over typical DC magnetron sputtering (MS) coatings, in terms of SRF performance.

In light of this, two series of multilayer SIS film coatings, with a Nb-AlN-NbN structure, were deposited onto electropolished OFHC Cu samples, with the use of HiPIMS, in order to determine the efficacy of this approach. This contribution details the development of these coatings and the required optimization of the coating parameters of the separate material systems, through the use of multiple material and superconducting characterization techniques. This research culminated in the deposition of two SIS-film quadrupole resonator (QPR) samples, using the final optimized coating process.

INTRODUCTION

The ever-increasing performance of bulk Nb cavities is pushing them towards their theoretical limits. The use of superconductor-insulator-superconductor (SIS) film structures has been proposed as one of the main pathways to overcome this [1]. Initial trials of this approach have indicated its potential for enhancing the penetration field above the H_{c1} of Nb [2]. These structures were originally envisaged for use with bulk Nb cavities. However, it is conceivable to combine the benefits of SIS structures with the benefits of coated Cu cavities, such as operation at 4.2 K. The use of SIS film coatings can also potentially delay the onset of the Q-slope typically observed with coated Cu cavities.

It is also clear that the use of, so-called, energetic deposition techniques such as high power impulse magnetron sputtering (HiPIMS), provide significant benefits over typical DC magnetron sputtering (MS) coatings, in terms of SRF performance, as has been shown for NbN thin films [3].

The results of investigations into HiPIMS-deposited multilayer SIS films are presented in this contribution. Each of the individual layers were previously optimised in separate studies. Given the predictions for an optimum shielding layer thickness [4] and feedback on initial quadrupole resonator (QPR) sample results [5], both the AlN and NbN layer thicknesses were adjusted during this study.

EXPERIMENTAL

Two series of multilayer SIS film coatings, with a Nb-AlN-NbN structure, were deposited onto electropolished OFHC Cu substrates and Si witness samples with HiPIMS, using a Nb (RRR 300) target in a commercial, high-volume, fully automated coating tool (CemeCon CC800). The HiPIMS parameters were kept constant at 1000 Hz and 120 µs for both the deposition of Nb and NbN in all coatings, in conjunction with a constant DC substrate bias. The AlN layer was deposited with DC MS, similar to the films detailed in [6]. A substrate temperature of 180°C was maintained during the coating of all three layers. The Nb and AlN layers were deposited with 100 % Ar (99.999 Vol-%) and N_2 (99.999 Vol-%) gas respectively, while the NbN layer was deposited with a mixture of Ar and N_2 with the N_2/Ar gas ratio maintained by flow rate control. A schematic of the film coating is shown in Fig. 1.

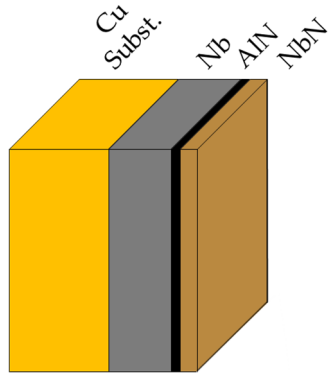

Figure 1: Schematic representation of the SIS film coating.

Prior to deposition, the system was baked at 650°C for 6 hours, to assist in removing any built up adsorbents, and thereafter evacuated to a base pressure of 6 x 10^{-7} mbar. The system was then backfilled with Ar to a pressure of

† stewart.leith@uni-siegen.de

ISBN: 978-3-95450-233-2 ISSN: 2673-5504 doi:10.18429/JACoW-SRF2021-SUPFDV012

1.5 x 10^{-3} mbar for target plasma cleaning and MF etching of the substrates. The samples were then coated in a single run, without removal from the deposition chamber.

During the deposition of the NbN layer in the first series of SIS film coatings, the turbopump was maintained at a decreased speed, owing to the higher pressure requirements. This resulted in pressure fluctuations and was adjusted to normal speeds, but equal pressure levels, for the second series of SIS film coatings. Besides this change, all films were deposited with the same deposition parameter settings, the only variable being the coating duration, which resulted in changing thicknesses of the AlN and NbN layers. The AlN layers were deposited with a thickness of either ~ 10 or ~ 30 nm while the NbN layers were varied between 75 and 232 nm. In order to ensure a consistent thickness for the two outer layers of the SIS films (AlN and NbN), the substrate holder was set to oscillate back and forth in front of the Nb target between – 10° and + 10°. The effects of the oscillations were quantified with SEM and XRD studies prior to the start of SIS film coatings and are not detailed here. The coating parameters for each of the films are detailed in Table 1.

Table 1: Deposition Parameter Values Used for Each of the Three Materials During the SIS Film Coatings

Material	Cathode Power (W)	Deposition Pressure (mbar)	Substrate Bias (V)	N_2 Content (%)
Nb	400	8.0 x 10^{-3}	50	0
AlN	3500	6.0 x 10^{-3}	0	100
NbN	400	2.2 x 10^{-2}	50	10

Following the deposition of the two series of SIS films, they were each analysed using a number of characterisation methods, including: AFM, CLSM, EDX, SEM, TEM and XRD as well as VSM and AC susceptometry magnetisation measurements.

RESULTS AND DISCUSSION

The results detailed here pertain to the HiPIMS SIS films deposited onto the electropolished Cu substrates. For all coatings, the Nb base layer thickness was maintained at ~ 3.2 µm, in line with results and conclusions from [7].

Similar to the previous DC MS SIS films [6], the surfaces of the HiPIMS SIS films are characterised by a multitude of different grain structures. However, this does not necessarily affect the structure of the NbN grains, which appear as if they are superimposed on top of the Nb film structure. The NbN layer is constituted by rounded, nanocrystalline grain peaks, as opposed to the sharp features present in the DC MS SIS films. This reduces the likelihood of flux enhancement and subsequent penetration. These features are visualised in Figure 2.

Image (a) displays an overview of a typical SIS film surface microstructure, while the images (b-x) display magnified views of the different apparent NbN layer grain structures. It is evident that the underlying HiPIMS Nb film plays a dominant role in the overall surface topography. However, the NbN grains themselves appear to have a similar nanocrystalline microstructure, regardless of the underlying Nb grain morphology. This surface topography is similar for all HiPIMS SIS films detailed here. Furthermore, due to the rounded nature of the NbN grain peaks, and consistent with the results of the individual HiPIMS NbN films [3], these HiPIMS SIS films display lower surface roughness values compared to the previously deposited DC MS SIS films [6].

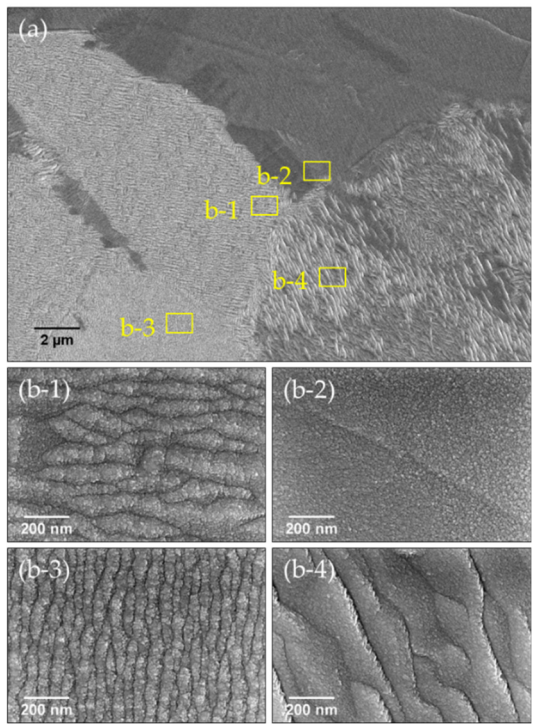

Figure 2: SEM images of the typical surface microstructure of HiPIMS based SIS films. (a) Overview image showing multiple grain structures. (b) Magnified images showing NbN microstructure grown on different Nb grain structures.

The effects of the different Nb grain morphologies are further evident in the cross-section images of these films, shown in Figure 3. Image (a) presents an overview and magnified view of a sample deposited with a 9 nm AlN interlayer, while image (b) displays a sample deposited with a 29 nm AlN interlayer. The NbN film grown on the undulating Nb surface is characterised by a Zone T microstructure, while those grown on relatively flat Nb surfaces show dense columnar structures, indicating the significant influence of the underlying Nb film. This is apparent regardless of the AlN layer thickness. Nevertheless, the films display an increased density compared to those deposited with DC MS as well as an improved surface topography, with RMS surface roughness values averaging 10.75 ± 1.67 nm compared to 13.67 ± 1.87 nm for DC MS deposited SIS films.

TEM investigations, displayed in Figure 4, revealed no interfacial voids between the HiPIMS Nb base layer and the Cu substrate or between the subsequent Nb/AlN and AlN/NbN layers. The layers display coherent, epitaxial growth on top of one another, as evidenced by the FFT image inset. This relationship is attributed to a

ISBN: 978-3-95450-233-2 ISSN: 2673-5504 doi:10.18429/JACoW-SRF2021-SUPFDV012

NbN(111)/AlN(111) relationship, as previously documented by Wen *et al* for thin AlN layers [8].

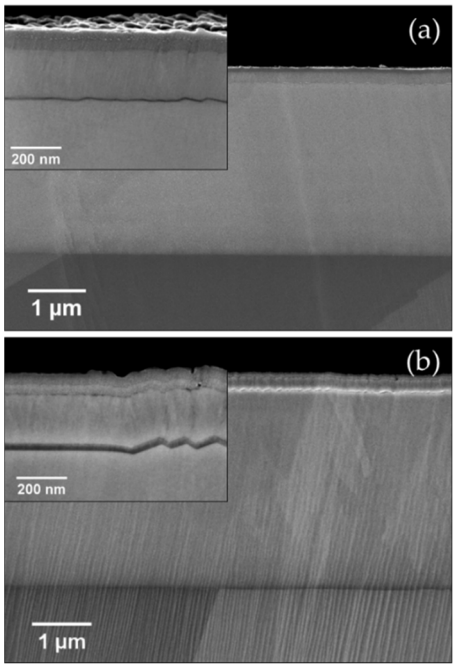

Figure 3: SEM images of the cross sections of two SIS films deposited on Cu with AlN layer thicknesses of 9 nm (a) and 29 nm (b) respectively. The observed top layer is due to re-deposition following Ar^+ ion polishing.

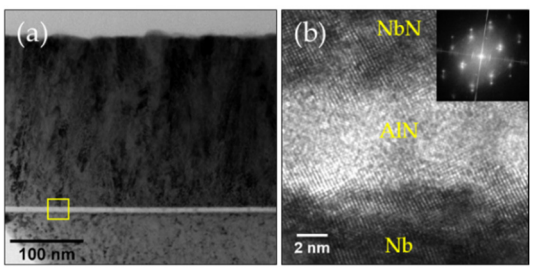

Figure 4: (a) TEM BF image of the SIS film coating. (b) HRTEM image of the interface between the three SIS film layers with corresponding FFT image inset. Imaged position in (b) indicated in (a).

The effect of the HiPIMS-related film density improvements was immediately apparent in the STEM EDX measurements completed on the SIS films, presented in Figure 5. As opposed to the results found with previous DC MS SIS films, where oxygen was found to have penetrated between the individual Nb grains, there is no presence of oxygen within the outer HiPIMS NbN film. The oxygen signal present on the surface of the SIS film is due to the glue used in TEM sample preparation. The lack of oxygen was further observed with SIMS investigations, not shown here, which displayed a significant reduction in the NbO^+ signal in the NbN layer compared to previous DC MS SIS films. The layers also display sharp contrast at the respective interfaces with no apparent intermixing.

The magnified XRD spectra of the individual HiPIMS NbN layer, on which the SIS films are based, and two representative SIS films, with AlN layer thicknesses of 9 nm

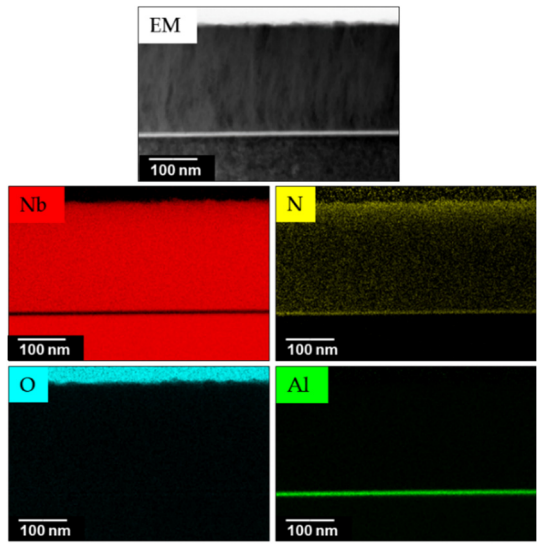

Figure 5: STEM EDX mapping results from a representative HiPIMS SIS film sample, displayed in atom percent.

and 29 nm respectively, are displayed in Fig 6. Because of the initial deposition pressure instabilities, the XRD spectra for the first HiPIMS SIS film series, not shown here, showed a NbN phase transition, from a cubic δ-NbN preferred film to a hexagonal Nb_5N_6 preferred film. This can only be attributed to the effects of deposition pressure fluctuations during coating as this effect disappeared with resolution of these instabilities.

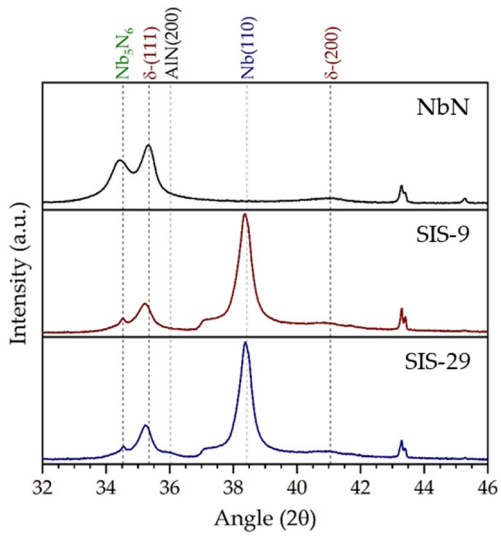

Figure 6: Magnified XRD spectrum of the base NbN film and two indicative SIS films deposited with a 9 nm and 29 nm thick AlN interlayer respectively.

The second series of SIS film coatings display NbN peaks in line with the results of the individual layer HiPIMS NbN sample used to deposit the SIS samples, regardless of the AlN layer thickness. These NbN films, individual and SIS, display a *δ*-NbN (111) preferred orientation with evidence of the hexagonal Nb_5N_6 phase.

All of the NbN films in these SIS samples display a negative shift of the δ-NbN (111) peak position (~ 35.2°) compared to the NbN film on which they are based [3]. This is

ISBN: 978-3-95450-233-2 ISSN: 2673-5504 doi:10.18429/JACoW-SRF2021-SUPFDV012

more pronounced for the first series of films, which display a preferred Nb_5N_6 phase formation and a subsequent lattice parameter of 4.4527 Å, which is outside the bounds defined for δ-NbN (4.38 - 4.42 Å [9]). The second series of films, which display an average lattice parameter of 4.4117 Å, lie near the upper bound defining δ-NbN. This is indicative of a significantly increased stress state and is likely due to the reduced thickness of these films compared to the individual layers and the improved NbN film density, allowing for stress transfer between the columnar grains. The DC MS NbN films deposited in previous SIS films possessed disjointed columnar structures, which allowed for significant stress relaxation.

The underlying Nb films are characterised by the Nb (110) peak, seen at $2\theta = 38.42°$, whose relative intensity indicates a Nb (110) preferred orientation, similar to the optimised Nb film detailed in [7]. The AlN interlayer is again characterised by its AlN (200) peak at ~ 36°, indicating formation of the sought after phase, and as expected, is more apparent in the SIS films with a thicker AlN layer.

In order to better determine the T_c of the NbN shielding layer, the SIS films were tested in an AC susceptometer. The normalised results of these measurements are presented in Fig. 7 (a). For the sake of brevity, only the results for the second, more stable series of films are presented.

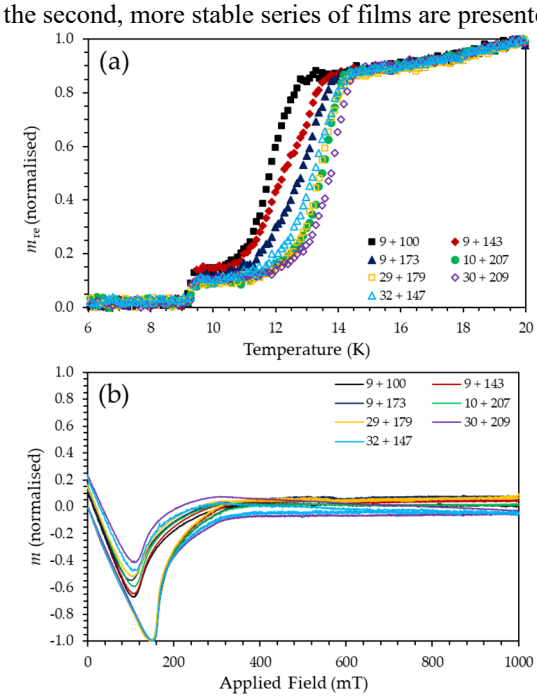

Figure 7: Superconducting results for the second set of HiPIMS SIS films. (a) displays the normalised real component of the AC susceptometry measurements, detailing the transition temperatures of both the Nb and NbN layers (b) displays sections of the normalised magnetisation loops.

As shown in [3], the T_c of HiPIMS NbN shows a significant lattice parameter dependence, with the T_c decreasing for increases of the lattice parameter above ~ 4.396 Å. As a result of this, the T_c's of the NbN layers in these SIS films, the highest being 14.48 K, are slightly reduced compared to that found with the individual layer (14.6 K). In line with this, the T_c's of the second series are markedly higher than those of the first series, for equal NbN and AlN thicknesses.

The results also indicated the influence of the AlN layer thickness on the NbN T_c. The NbN films deposited onto the ~ 30 nm thick AlN interlayer showed higher T_c values, for equal or similar NbN layer thicknesses, than those deposited onto the ~ 10 nm thick AlN interlayer. Finally, regardless of the pressure fluctuations or AlN layer thickness, the NbN T_c displayed a marked dependence on the layer thickness, increasing with increasing thickness, in line with previous SIS film samples [6]. The T_c's of all HiPIMS SIS films are detailed in Fig. 8.

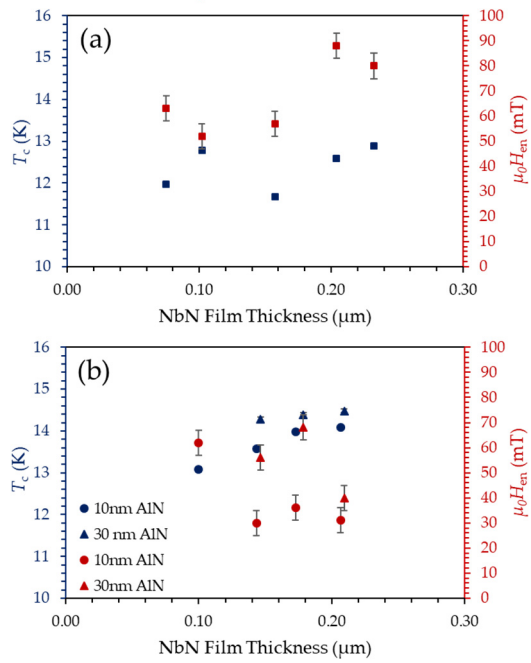

Figure 8: Superconducting transition temperature and entry field values as a function of NbN film thickness for the two series of HiPIMS SIS films. (a) Pertains to series 1, deposited with a fixed 10 nm AlN layer thickness and (b) pertains to series 2, with the different AlN layer thicknesses indicated in the legend.

The virgin curve and reverse branch of the resultant magnetisation loops from VSM testing of the second series of SIS films are presented in Fig. 7 (b). In contrast to series 1, not shown here, the virgin curve of the second series maintains a smooth shape up to high fields. Further to this, the samples deposited in series two possess far narrower magnetisation loops compared to series one, indicative of a lower amount of trapped flux [10]. Both series of films present a pronounced dip in the reverse branch, which is significantly more noticeable in series two, indicating an improved surface barrier condition. Interestingly, the amount of trapped flux increased with both an increase in the AlN layer thickness and an increase in NbN thickness.

The two series of HiPIMS SIS films show a noticeable divide when comparing their entry field data, obtained with a 2% difference criterion from the initial linear slope of the Meissner shielding state. The films deposited in the first series show a consistently higher H_{en}, even at low NbN film

ISBN: 978-3-95450-233-2 ISSN: 2673-5504 doi:10.18429/JACoW-SRF2021-SUPFDV012

thickness, with lower variability. The highest $H_{en} = 88.0 \pm 4.4$ mT of all HiPIMS SIS samples was achieved for this series. This is an interesting result, given the preferred formation of the Nb_5N_6 phase in these films.

The second series of films hints at a further split in the results based on the AlN thickness, with the three films coated with a 30 nm AlN interlayer showing consistently higher H_{en} values compared to those deposited with a 10 nm interlayer, though more results and further test methods are required to confirm this. The different series and different AlN thickness resulted in separate NbN thicknesses corresponding to peak entry field values. This value ranges from 173 nm for the 10 nm AlN samples to 204 nm for the series 1 films, higher than that proposed by Kubo for NbN-based SIS films [4]. The reasoning behind these differences is likely linked to the NbN phase formation.

CONCLUSION

The deposition of HiPIMS-based SIS films onto Cu substrate have been successfully accomplished during this study, with the results indicating their efficacy. The results further display the significant benefits which accompany the use of HiPIMS, specifically the significant densification of the outer NbN shielding layer and the reduction of the surface roughness. These two results are also likely the reasons behind the low amount of trapped flux observed in VSM testing of the second series of these films.

The results of this study also presented possible routes for improvements of future coatings as well as further analysis techniques. The increased lattice parameter values, which likely resulted in the decreased NbN T_c, indicate a heightened state of stress in the films compared to the individual NbN films and point to a potential optimisation pathway.

Finally, but most importantly, even though the SIS films displayed lower H_{en} values than the individual Nb layers on which they are based, the SIS film samples in series two possess the smallest magnetisation loops and lowest amount of trapped flux of all SIS films, even lower than previous HiPIMS Nb samples [7]. It is thus important to obtain an understanding of the relationship between the entry field and the size of the magnetisation loops in terms of what to focus on for future coating optimisation. Efforts towards understanding the SRF performance of SIS film coatings were pursued with the deposition of two final QPR samples with the same HiPIMS SIS film coatings, albeit with different AlN layer thicknesses. The results of this effort are detailed in [11].

ACKNOWLEDGEMENTS

This work forms part of the EASITrain Marie Sklodowska-Curie Action (MSCA) Innovative Training Networks (ITN) which has received funding from the European Union's H2020 Framework Programme under Grant Agreement no. 764879.

The superconducting characterisation measurements were completed within the European Union's ARIES collaboration H2020 Research and Innovation Programme under Grant Agreement no. 730871

Part of this work was performed at the Micro- and Nanoanalytics Facility (MNaF) of the University of Siegen.

REFERENCES

[1] A. Gurevich, "Enhancement of rf breakdown field of superconductors by multilayer coating," *Appl. Phys. Lett.*, vol. 88, no. 1, p. 012511, Jan. 2006. doi:10.1063/1.2162264

[2] C. Z. Antoine *et al.*, "Optimization of tailored multilayer superconductors for RF application and protection against premature vortex penetration," *Supercond. Sci. Technol.*, vol. 32, no. 8, p. 085005, Aug. 2019. doi:10.1088/1361-6668/ab1bf1

[3] S. Leith, M. Vogel, B. Bai, X. Jiang, E. Seiler, and R. Ries, "HiPIMS NbN Thin Film Development for use in Multilayer SIS films," presented at the 20th Int. Conf. on RF Superconductivity (SRF'21), Lansing, Michigan, USA, July 2021, paper SUPFDV013, this conference.

[4] T. Kubo, "Multilayer coating for higher accelerating fields in superconducting radio-frequency cavities: a review of theoretical aspects," *Supercond. Sci. Technol.*, vol. 30, no. 2, p. 023001, Feb. 2017. doi:10.1088/1361-6668/30/2/023001

[5] A. Gurevich *et al.*, "ARIES QPR SIS Film Feedback Session," private communication, 2020.

[6] S. Leith *et al.*, "Superconducting NbN thin films for use in superconducting radio frequency cavities," *Supercond. Sci. Technol.*, vol. 34, no. 2, p. 025006, Feb. 2021. doi:10.1088/1361-6668/abc73b

[7] S. Leith *et al.*, "HiPIMS deposition of Nb thin films onto Cu substrates," to be published.

[8] M. Wen *et al.*, "The AlN layer thickness dependent coherent epitaxial growth, stress and hardness in NbN/AlN nanostructured multilayer films," *Surf. Coatings Technol.*, vol. 235, pp. 367–375, Nov. 2013. doi:10.1016/j.surfcoat.2013.08.004

[9] C. Stampfl *et al.*, "Electronic structure and physical properties of early transition metal mononitrides: Density-functional theory LDA, GGA, and screened-exchange LDA FLAPW calculations," *Phys. Rev. B*, vol. 63, no. 15, p. 155106, Mar. 2001. doi: 10.1103/PhysRevB.63.155106

[10] D. M. Gokhfeld, "Analysis of Superconductor Magnetization Hysteresis," *J. Sib. Fed. Univ. Math. Phys.*, vol. 11, no. 2, pp. 219–221, May 2018. doi: 10.17516/1997-1397-2018-11-2-219-221

[11] D. Tikhonov *et al.*, "Investigation of SIS multilayer films at HZB," presented at the 20th Int. Conf. on RF Superconductivity (SRF'21), Lansing, Michigan, USA, July 2021, paper SUPFDV006, this conference.